Proceedings of the 20th International Conference on Soil Mechanics and Geotechnical Engineering– Rahman and Jaksa (Eds)

Evaluation of residual strength characteristics of reconstituted volcanic soil at Atsuma town, Hokkaido with stacked-ring shear tests

Évaluation des caractéristiques de la résistance résiduelle du sol volcanique reconstitué dans la ville d'Atsuma, à Hokkaido, à l'aide d'essais de cisaillement à anneaux superposés.

Kenji Watanabe, Hiroyuki Kyokawa, Tomoya Onodera & Junichi Koseki
Department of Civil Engineering, University of Tokyo, Japan, watanabe@civil.t.u-tokyo.ac.jp

Yudai Aoyagi
Department of Civil Engineering, University of Tokyo, Japan (currently Public Works Research Institute)

ABSTRACT: During the 2018 Hokkaido Eastern Iburi earthquake, slope failures with a large distance sediment flow have been observed at many places, despite the gentle slope having a slope of about 10 to 15 degree. These phenomena are thought to be caused by the existence of "volcanic ash soil", but the details have not been understood yet. The objective of this study is to investigate the reasons of the large-scale collapse of the gentle slope observed in the earthquake. In this study, using the newly developed "stacked-ring shear test apparatus", the residual strength characteristics in the large strain level (about 1000%) were evaluated for seven types of volcanic ash soil collected in the field survey at Atsuma town, Hokkaido. As a result, it was confirmed that this volcanic ash soil showed large strain softening behavior as compared with ordinary soil, and showed extremely low residual strength (about 5 to 10 kPa) especially in the large shear strain level. Simple stability analysis of a gentle slope using the residual strength measured in this test showed that the slope could not sustain its own weight even after the earthquake. This indicates the possibility of large-scale collapse of gentle slopes.

RÉSUMÉ : Lors du séisme d'Hokkaido Eastern Iburi de 2018, des ruptures de pente avec un flux de sédiments sur une grande distance ont été observées à de nombreux endroits, bien que la pente douce ait une inclinaison d'environ 10 à 15 degrés. On pense que ces phénomènes sont causés par l'existence d'un "sol de cendres volcaniques", mais les détails n'ont pas encore été compris. L'objectif de cette étude est de rechercher les raisons de l'effondrement à grande échelle de la pente douce observée lors du tremblement de terre. Dans cette étude, en utilisant le nouvel "appareil de test de cisaillement à anneaux empilés", les caractéristiques de la force résiduelle dans le niveau de déformation important (environ 1000%) ont été évaluées pour sept types de sol de cendres volcaniques collectées dans l'enquête de terrain dans la ville d'Atsuma, Hokkaido. Comme résultat, il a été confirmé que ce sol de cendre volcanique a montré un comportement de ramollissement de grande déformation par rapport au sol ordinaire, et a montré une force résiduelle extrêmement basse (environ 5 à 10 kPa) particulièrement dans le niveau de grande déformation de cisaillement. L'analyse simple de stabilité d'une pente douce utilisant la force résiduelle mesurée dans ce test a montré que la pente ne pourrait pas soutenir son propre poids même après le tremblement de terre. Cela indique la possibilité d'un effondrement à grande échelle des pentes douces.

KEYWORDS: slope stability, volcanic ash soil, residual strength, stacked-ring shear test.

1 INTRODUCTION

Many seismic-induced large-scale landslides and slope failures in a region having deep deposit of volcanic ash soil in Japan have been reported till now. Over the past few years, in the 2016 Kumamoto earthquake and the 2018 Hokkaido Eastern Iburi earthquake, several landslides of which runout distance reaches over 100m at gentle slopes less than 10-15 deg were observed (Kawamura, 2019). It has been considered that one of major reasons for such landslide phenomena is the existence of volcanic ash soil (Chiaro, G. et al, 2017). However, the conventional soil testing apparatuses cannot properly evaluate the shear characteristics at large strain level, which subject to soil in the sliding plane, due to their mechanical constraints. Thus, the large-scale landslide at gentle slope of volcanic ash soil is not yet well understood.

Authors conducted the field survey on the 2018 Hokkaido Eastern Iburi earthquake and observed that muddy volcanic ash clayey soil with higher water content is stretched widely on the surface of sliding plane of the landslides. In this study, a series of simple shear tests on the reconstituted samples obtained from the large-scale landslide site was carried out, and the large deformation characteristics including the residual strength, which is used in slope stability analysis, are discussed. The tests were conducted using the stacked-ring shear apparatus (Seto et al. 2016), which can continuously apply shear displacement over 1000% of shear strain and replicates the simple shear condition before the peak strength.

2 OBJECTIVE OF THIS STUDY

2.1 *Importance of evaluation of residual strength*

In order to evaluate the stability of a slope, the residual strength of target soil layers is often used in slope stability analysis. Based on the shaking table tests, Shinoda et al (2015), classified the seismic-induced failures of a slope into three patterns: first, the sliding soil mass collapses immediately after the destabilization of a slope, and secondly, the deformation gradually progresses after the destabilization of a slope and the sliding failure finally occurs, and thirdly, although the deformation develops after the destabilization of a slope, that deformation stops when earthquake ends. Moreover, below sequence of events on the sliding soil mass was experimentally explained: the shear strength acting along a failure plane decreases to the residual strength with development of deformation, and if the strength is not enough to sustain the weight of soil mass, i.e., critical seismic intensity is zero or nearly zero, the sliding soil mass

instantaneously collapses. Considering these experimental results, therefore, it can be deduced that first or second type of failure occurred at the large-scale sliding at the gentle slope in Atsuma due to the 2018 Hokkaido Eastern Iburi earthquake. In order to verify such consideration, however, the evaluation of the strength characteristics of the soil layer triggering the sliding, especially the residual strength at large shear displacement (strain) level, are necessary.

2.2 *Evaluation method of the residual strength*

The residual strength of soil only depends on the particle size and shape, and mineral composition. It can be uniquely determined by the stress level regardless of the stress history. Moreover, undisturbed sample and disturbed (reconstituted) sample exhibit the same residual strength. However, quite large shear displacement is required to achieve the residual stress state in the direct shear test and the ring shear test (Skempton, 1985). On the other hand, because of easiness of molding an undisturbed sample and handling an apparatus, a triaxial shear test is often performed to evaluate the residual strength, but a general triaxial shear apparatus can apply a few dozen percent of strain. Additionally, the direct shear test and the ring shear test predetermining the shear plane cannot replicate the simple shear condition in the apparatus. Therefore, such conventional testing apparatus would not be proper for evaluating the shear characteristics over a wide range of strain.

With such backgrounds, a new testing apparatus which can conduct the monotonic simple shear with over 1000% of shear strain is used in this study. Unlike general direct shear test and ring shear test apparatuses, this new apparatus holds a specimen by several number of hollow cylindrical stacked rings instead of a membrane, and it results in successfully replicating the simple shear behavior before the emergence of shear bands in the specimen. The simple shear tests were conducted on eight samples in total including 7 types of volcanic ash soils obtained from the site of the slope failure in Atsuma town due to the 2018 Hokkaido Eastern Iburi earthquake, and Inagi sand which is mountain sand, by the stacked-ring shear apparatus in this study. The shear strain greater than 1000%, in which the residual strength can be observed, was applied to the specimen to investigate the large deformation characteristics of various volcanic ash soils.

3 TEST APPARATUS

The outline of the stacked-rings shear apparatus is shown in Figure 1. It consists of three parts: a pneumatic system part using two bellofram cylinders for the axial stress, a direct motor system part for the torsional shear stress, and a stacked-rings part. The stacked-rings part consists of 11 rigid rings, having a thickness of 5 mm each. The bottom ring is located 2 mm below the top of the pedestal, so that the height of the specimen is 53 mm, while the inner and outer diameters of the specimen are 90 mm and 150mm. Those rigid inner and outer parts of the stacked-rings can support a hollow cylindrical specimen. Metal bearings are installed in between the outer and inner rings, respectively, so the friction in circumferential direction of each ring can be reduced as minimum as possible. A pair of two-component load cells, which can measure the vertical and torsional stress independently, are attached to the upper and lower ends of the hollow cylindrical specimens.

Due to the vertical friction between the stacked-rings and the specimen, a vertical stress at the bottom of the specimen is approximately 60% of the vertical stress at the top of the specimen. In this study, the stress-strain relationship and stress paths are evaluated by using the average value of the vertical

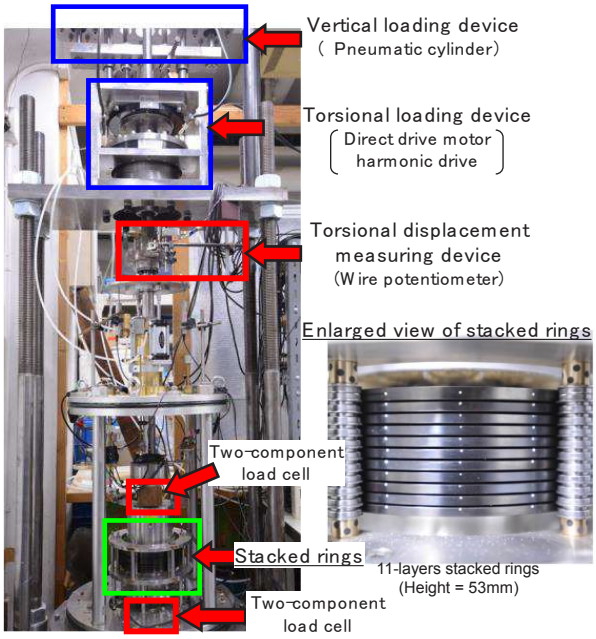

Figure 1. Outline of stacked-rings shear apparatus.

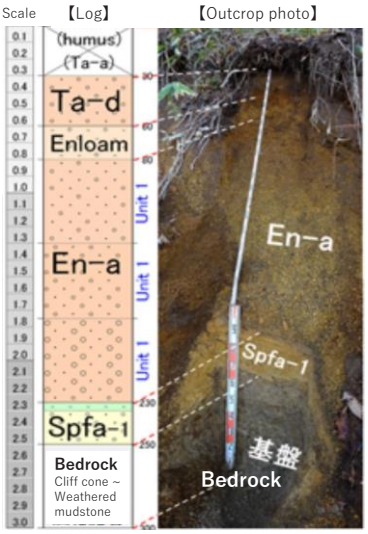

Figure 2. Stratigraphy of volcanic soil at Atsuma town (around the Mizuho Dam, Chimoto et al., 2020).

stress and torsional shear stress. Assuming that stress distribution is linear throughout the specimen height direction, the average values can be considered as the values at the center of the specimen height. In this apparatus, both lateral and radial stresses on the stacked-rings are not measured, while the shear displacement in torsional shear loading is measured using a wire-type potentiometer attached on the side of the loaded shaft.

4 MATERIAL USED FOR THE STUDY

4.1 *Volcanic soil distributed in the Atuma region of Hokkaido*

In Atsuma Town, volcanic soil named Tarumae (Ta-d), Eniwa (En-a), and Shikotsu (Spfa-1) are deposited thickly in parallel from the top, and Andosols layer and loam layer are deposited between them (Chimoto et al., 2019). These layers were formed during volcanic eruptions about 9,000 years ago, about 20,000

Table 1. Length, width and slope angle of each site.

Site	Conditions of slope failures		
	Length (m)	Width (m)	Slope angle θ(°)
Horosato 1	54	45	17
Horosato 2	210	30	-
Sakuragaoka	99	73	19
Asahi	87	70	10
Takaoka	39	68	22

years ago, and about 40,000 years ago, respectively. These tephras are characterized by coarse particles, low density, and large void. Figure 2 shows the stratigraphy around the Mizuho Dam as an example of a typical local stratigraphy. Due to the thickness of the fall after the eruption and the effects of weathering and erosion after that, the thickness and distribution of each layer differ from region to region, and slope failures occurred in different layers depending on the region.

4.2 *Soil sampling*

Among the different type of volcanic soil such as shown in Figure 2, soil samples of Ta-d and loam layer on En-a (hereinafter referred to as Enloam) were collected from the field survey in the Horosato, Asahi and Sakuragaoka areas with disturbed condition. In addition, soil sample of the Spfa-1 layer was collected in Takaoka area, which is about 8 km north of Horosato. In the field survey, hand vane tests and simple dynamic cone penetration tests were conducted and an undisturbed sample were collected by thin-walled sampler. Furthermore, the wet density and water content were measured by a cylindrical sampler and these values were reflected in the preparation of specimens for laboratory tests.

Table 1 shows the length, width and angle of failure of sliding area at each field survey area, and Figure 3 shows overview of the Asahi area and Sakuragaoka area. There are two types of Ta-d layer, reddish brown pumice and yellowish-brown cohesive soil, which are collected at a depth of about 1.4 m and about 3.0 m from the surface layer, respectively (hereinafter, Ta-d reddish brown, Ta-d yellowish brown). For comparison, the laboratory

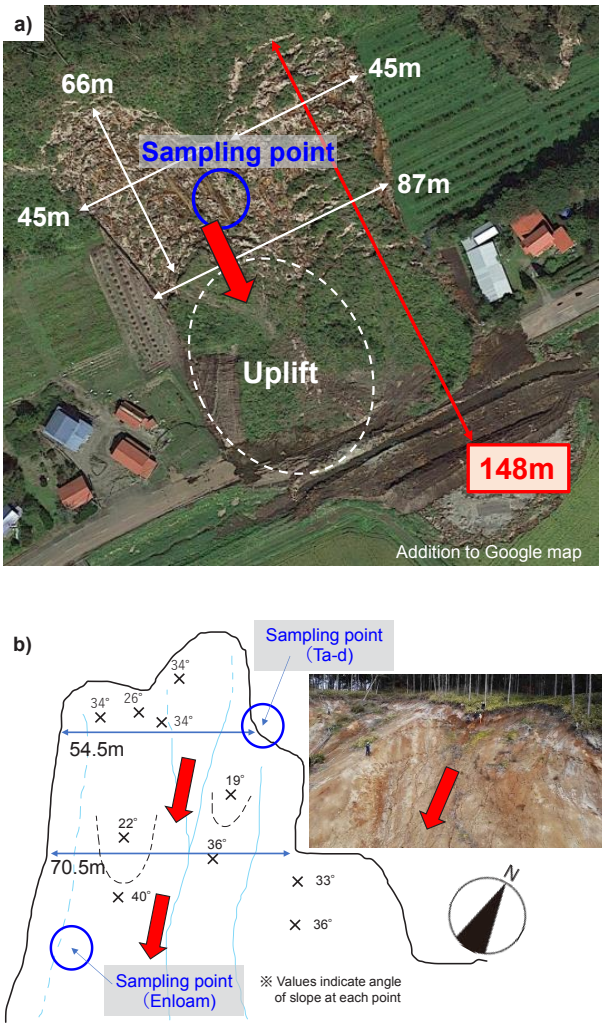

Figure 3. Overview of land slide and sampling point (a: Asahi area, b:Sakuragaoka area).

Table 2. Physical properties of each sample and conditions for specimen preparation

No	Site name	Layer name	Soil particle density (g/cm³)	In-situ water content (%)	In-situ dry density (g/cm³)	Consistency indexes w_L (%)	Consistency indexes w_P (%)	Consistency indexes I_P	Fines content F_c [%]	Specimen for torsional tests: Dry density (g/cm³) Before consolidation	Specimen for torsional tests: Dry density (g/cm³) After consolidation	Specimen for torsional tests: Initial water content (%)
1	Horosato 1	Enloam	2.71	57.6	0.89	60.3	48.4	11.9	29.0	0.89	0.94	57.6
2	Sakuragaoka	Enloam	2.75	84.8	0.77	65.2	53.7	11.5	42.8	0.77	0.84	84.8
3	Horosato 2	Ta-d (reddish)	2.68	189.1	0.34	169.2	139.5	29.7	20.0	0.37	0.39	224.4
4	Asahi	Ta-d (reddish)	2.75	107.4	-	141.6	131.1	10.5	8.1	0.70	0.72	78.1
5	Asahi	Ta-d (yellowish)	2.76	89.2	0.805	103.1	70.8	32.3	67.7	0.79	0.83	87.1
6	Sakuragaoka	Ta-d (yellowish)	2.73	212.9	0.51	137.3	112.6	24.7	69.3	0.38	0.41	212.9
7	Takaoka	Spfa-1	2.55	107.7	0.59	49.0	40.0	9.0	39.9	0.59	0.62	93.3
8	-	Inagi sand	2.71	—		—	—	—	4.8	1.44		18.5

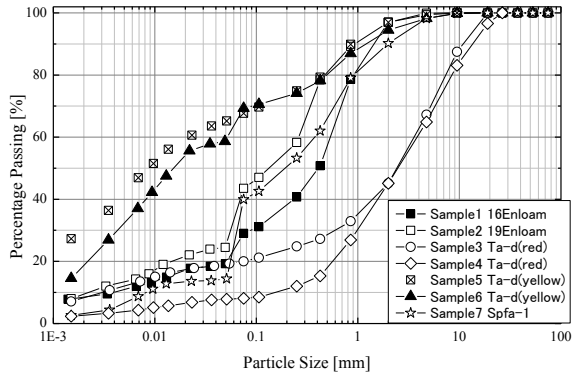

Figure 4. Grain size distribution of each samples.

test is also conducted using mountain sand (Inagi sand) collected in the Kanto region (near Tokyo). Figure 4 shows the grain size distribution curves of eight types of samples, and Table 2 shows the physical properties of each sample and the conditions for specimen preparation.

5 TESTING PROCEDURE AND RESULTS

5.1 *Specimen preparation and loading condition*

A monotonic loading test was performed on eight types of samples (Table 2) under constant volume state (equivalent to undrained state) using the stacked-rings shear apparatus. The specimen was prepared to have the same wet density and the water content as measured at each site. The specimen was divided into 5 layers in the height direction and prepared by a wet tamping method. Samples No.1 to No.6 were first air-dried in a desiccator containing silica gel, and then adjusted to have the same water content as the site. For sample No.7, the specimen was prepared by the wet compaction method so that the sample collected in the field had the target density without adjusting the water content. The right column of Table 2 also shows the dry density and water content of the specimens after preparation. It can be seen that the dry density and water content measured by the cylindrical sampler in the field survey could not be perfectly reproduced by the wet compaction method in the laboratory in some cases.

For sample No.8 (Inagi sand), the specimen was prepared with a dry density of 1.44g/cm^3 and water content of 18.5%, which corresponds to 85% of the maximum dry density (ρ_{dmax}=1.689g/cm^3) and an optimum water content determined by the compaction test (standard proctor).

After the preparation of the specimen, the vertical stress of 50 kPa, which corresponds to the overburden pressure at about 2 to 3 m depth, was applied to the top of the specimen to perform one-dimensional consolidation. The dry density after the one-dimensional consolidation is also shown in Table 2. After reaching a predetermined stress state, the specimens were subjected to monotonic loading at a shear strain rate of 1.1%/min while the axial displacement was fixed for keeping the specimen height constant, namely constant volume condition. Monotonic loading was carried out until the shear strain reached 1000% (shear displacement of about 500 mm), and the vertical and shear stresses were measured by two-component load cells placed at the top and bottom ends of the specimen.

5.2 *Test results*

The stress path and stress-strain relationship obtained from the monotonic loading test are shown in Figures 5 and 6, respectively. First, the stress path shows that the three samples with high fines contents (No.2: Enloam, No.5: Ta-d yellowish brown, and No.6: Ta-d yellowish brown) exhibited negative dilatancy behavior throughout the test. On the other hand, the dilatancy behavior of No.1 (Enloam), No.3 (Ta-d reddish brown), No 4 (Ta-d reddish brown) and No.8 (Inagi sand) changed from negative to positive before reaching the peak strength, and the axial stress (confining pressure) turned from decreasing to increasing under constant volume conditions. This behavior was similar to the undrained shear behavior of normal overconsolidated clays. However, after reaching the peak state, both shear stress and axial stress decreased along the failure envelope. This "turn-down" behavior was similar to that

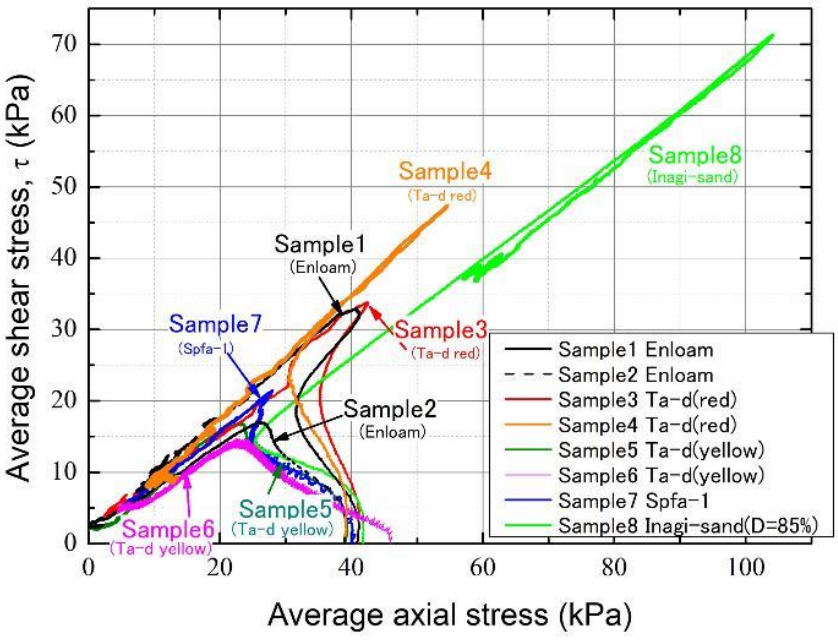

Figure 5. Stress path of each sample.

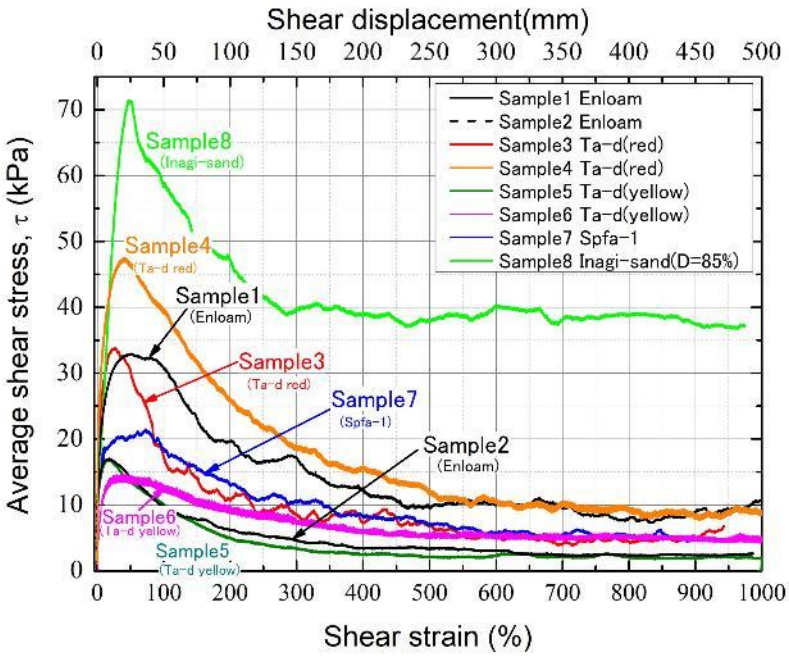

Figure 6. Stress-strain relationship of each sample.

observed in undrained shear test of structured naturally deposited clays, but the large stress reduction was the specific behavior of these samples.

The stress-strain relationship (Figure 6) shows that the peak strength of all specimens was mobilized at a shear strain level of 20-40%, followed by a gradual strain softening behavior, reaching the residual strength at a shear strain of 500% or more (shear displacement of 250-300mm or more). Skempton (1985) showed that a shear displacement of 100-500mm is required for clay to reach the residual state in the ring shear test, and the results obtained in this study were consistent with this finding. Note that the residual strength of the samples collected at the site (No.1 to 7) was about 5 to 10 kPa, while the Inagi sand (No.8) was about 40 kPa, not showing such a large softening behavior.

Figure 7 shows the rotational displacement of the staked-rings at each loading stage for samples No.3 and No.5. Both specimens exhibited almost uniform simple shear deformation in the pre-peak state, while the strain localization was observed in post-peak condition. For sample No.3, the shear deformation was mainly concentrated between the fourth and fifth ring from the bottom, while the rings above showed almost uniform rotational deformation. Clear cracks were observed between these rings during the process of removing the specimen, indicating that the shear strength mobilized at this height was mainly decreased in the post-peak state. On the other hand, uniform simple shear deformation behavior was observed even after peak state for sample No.5. Strain localization such as observed in sample No.3 was observed only after reaching large strain level, between the third and fourth ring from the bottom. This different shear deformation characteristic may have induced a more gradual strain softening behavior in sample No.5 compared to sample No.3.

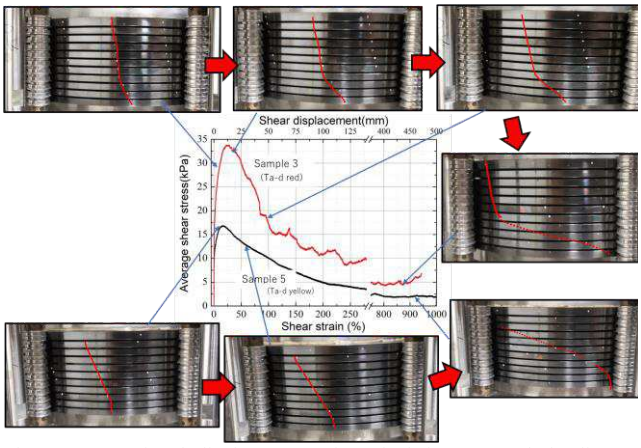

Figure 7. Rotational displacement of stacked-rings at each loading stage.

Table 3. Safety factors obtained by slope stability analysis.

		(1) Normal condition ($\tau=\tau_{peak}$, $k_h=0$)	(2) Seismic condition ($\tau=\tau_{peak}$, $k_h=0.98$)	(3) Post-seismic condition ($\tau=\tau_{res}$, $k_h=0$)
No.1	Enloam	4.68	0.71	1.42
No.3	Ta-d (reddish)	4.79	0.73	0.70
No.6	Ta-d (yellowish)	2.41	0.36	0.28
No.7	Spfa-1	3.12	0.47	0.71
No.8	Inagi sand	10.2	1.54	5.21

5.3 *Slope stability analysis*

Simple slope stability analysis was carried out using the shear strength obtained above. It was assumed that a linear failure plane at an angle of 10 degrees from the horizontal plane was formed at a depth of 2 m from the slope surface. The groundwater level was assumed to located far below the failure

plane. The shear strength which was obtained in both peak and residual state in Figure 6 were used in the stability analysis. Table 3 shows the safety factor (=shear resistance force/acting force) of the slope under the following three conditions;

(1) Normal condition (peak strength, k_h =0),

(2) Seismic condition (peak strength, k_h =0.98)

(3) Post-seismic condition (residual strength, k_h=0).

where, k_h is horizontal seismic coefficient. The value of k_h (=0.98) in seismic condition was derived from the recorded maximum acceleration (three-component composite) of 967.3 Gal during the 2018 Hokkaido Eastern Iburi earthquake in Kanuma, Atsuma-town (JMA, 2019), which is close to the site.

It can be seen from Table 3 that the safety factor at normal condition is larger than 1.0 for all samples, indicating that the slope was stable before the earthquake. However, the safety factor become less than 1.0 during the earthquake, indicating that the slope was destabilized by the earthquake and displacement along the failure plane started to occur. It should be noted that, for samples No.3, 6, and 7, the safety factors obtained from the residual strength are less than 1.0 even after the earthquake (k_h=0). This result indicates that gentle slope cannot sustain its own weight even after the earthquake when the soil supporting the slope exhibits an extreme strain-softening behavior such as observed in Figure 6. This result explain the possibility of large-scale instantaneous collapse of gentle slopes.

Such a large-scale slope failure due to low residual strength after an earthquake has been confirmed in previous shaking table model tests conducted by Shinoda et al (2015).

6 CONCLUSIONS

In this study, using the newly developed "stacked-ring shear test apparatus", the residual strength characteristics in the large strain level were evaluated for seven types of volcanic ash soil collected in the field survey at Atsuma town, Hokkaido.

As a result, it was confirmed that this volcanic ash soil showed large strain softening behavior as compared with other mountain sand, and showed extremely low residual strength, especially in the large shear strain level. Simple stability analysis of a gentle slope using the residual strength measured in this test showed that the slope could not sustain its own weight even after the earthquake. This indicates the possibility of large-scale instantaneous collapse of gentle slopes.

7 ACKNOWLEDGEMENTS

We would like to express our sincere gratitude to Mr. Yasuo Chomoto of Kiso-Jiban Co. for his support on the site investigation and sample collection in Atsuma area.

8 REFERENCES

Chiaro, G., Alexander, G., Brabhaharan. P., Massey, C., Koseki, J., Yamada, S. and Aoyagi, Y. 2017. Reconnaissance report on geotechnical and geological aspects of the 14-16 April 2016 Kumamoto earthquakes, Japan, Bulletin of the New Zealand Society for Earthquake Engineering, Vol. 50, No. 3, 365-393

Chimoto, Y., Toda, H. and Isogai, K. 2020. Overview of Tephra layer slides observed in the northern part of the land slide area, Landslides inducred by the 2018 Hokkaido Eastern Iburi Earthquake, 4.7, pp.156-162, Hokkaido University Press (in Japanese)

JMA 2019. Earthquake disaster report (2018 Hokkaido Eastern Iburi earthquake), Japan Meteorological Agency (in Japanese), https://www.jma.go.jp/jma/kishou/books/saigaiji/saigaiji_201901.pdf

Kawamura, S., Kawajiri S. Hirose, W. and Watanabe, T. 2019. Slope failures/landslides over a wide area in the 2018 Hokkaido Eastern Iburi earthquake, *Soils and Foundations*, Vol. 59, No.6, 2376-2395, https://doi.org/10.1016/j.sandf.2019.08.009

Shinoda, M., Watanabe, K., Sanagawa, T., Abe, K., Nakamura, H., Kawai, T. and Nakamura, S. 2015. Dynamic behavior of slope models with various slope inclinations, *Soils and Foundations*, Vol. 55, No.1, 127-142, https://doi.org/10.1016/j.sandf.2014.12.010

Skempton, A. W. 1985. Residual of clays in landslides, folded strata and the laboratory, Geotechnique 35, No.1, pp.3-18

Wahyudi, S. Koseki, J. Sato, T. and Chiaro, G. 2016. Multiple-Liquefaction Behavior of Sand in Cyclic Simple Stacked-Ring Shear Tests, International Journal of Geomechanics, Vol. 16, Issue 5